DEVELOPMENT OF AN AUTOMATIC DESIGN AND ANALYSIS TOOL FOR AXIAL FLOW COMPRESSORS

Necmettin Anıl KÜNDEŞ*, Mehmet Halûk AKSEL** and Özgür Uğraş BARAN***
* Orta Doğu Teknik Üniversitesi, Makina Mühendisliği Bölümü
06800 Çankaya Ankara, kundes@metu.edu.tr
** Orta Doğu Teknik Üniversitesi, Makina Mühendisliği Bölümü
06800 Çankaya Ankara, aksel@metu.edu.tr
*** Orta Doğu Teknik Üniversitesi, Makina Mühendisliği Bölümü
06800 Çankaya Ankara, ubaran@metu.edu.tr

Abstract: This paper presents a new design and analysis tool that is developed to be employed during the design process of axial flow compressors. The tool chain implemented by this design tool consists of five parts: a mean-line design tool, followed by a blade geometry parametrization tool. Then 3D blade geometry is created, next a high quality structured mesh is generated and completed by Computational Fluid Dynamics (CFD) solution. All components employed in the new tool are either new developments, or achieved by utilization of in-house solvers. Design process for a multistage axial flow compressor starts with the 1-D mean line design phase, followed by 2D design of the blade by employing radial equilibrium theory. 3D blade geometry is constructed by the mapping and stacking operations of the 2D blade cross-sections calculated and generated at the geometry parametrization tool by using geometric parameters of blade angles, chord lengths, blade thickness distributions, hub and shroud curves. These cross sections are defined with non-uniform rational B-spline (NURBS) curves for optimization objectives. In the solution part, an in-house developed multiblock structured mesh generation code is restructured to automatically generate mesh around the 3D blade. 3D CFD analyses are performed by an in-house solver on this grid. The design and solution cycle is validated by using NASA Rotor-37 compressor rotor test case. A new rotor blade is achieved with similar pressure-ratio with Rotor-37**.**
Keywords: Axial Flow Compressor, Mean Line Design, Parametrization, Radial Equilibrium Theory, Multiblock Structured Mesh Generation, CFD

EKSENEL KOMPRESÖRLER İÇİN OTOMATİK TASARIM VE ANALİZ ARACI GELİŞTİRİLMESİ

Özet: Bu makale, eksenel kompresörlerin tasarım aşamasında kullanılmak üzere geliştirilen bir tasarım ve analiz aracını sunmaktadır. Bu tasarım aracı birbiriyle uyumlu çalışan beş bölümden oluşmaktadır. Orta çizgi tasarım aracı, kanat geometrisini parametrik hale getiren bir araç ile devam eder. 3B kanat geometrisi oluşturulduktan sonra, yüksek kaliteli düzenli çözüm ağı oluşturulur. Ardından süreç Hesaplamalı Akışkanlar Dinamiği (HAD) çözümleri ile tamamlanır. Bu yeni araç dâhilinde yer alan tüm bileşenler ya yeni geliştirilmiştir ya da araştırma grubu içinde geliştirilmiş çözücülerden yararlanarak elde edilmiştir. Çok kademeli bir eksenel kompresör için tasarım süreci orta çizgi tasarım evresiyle başlar. Orta çizgi tasarımı 1B analizlerden oluşmaktadır. 2B kanat enine kesitleri kanat açıları, kiriş uzunlukları, kanat kalınlık dağılımları, göbek ve uç eğrileri kullanılarak oluşturulur. Optimizasyon amacı gözetilerek, bu enine kesitler düzgün olmayan rasyonel B-spline (NURBS) eğrileri ile tanımlanır. Tasarım, Radyal denge teorisi kullanılarak elde edilen 2B kanat tasarımı ile devam eder. 3B kanat geometrisi, 2B kanat enine kesitlerinin eşleştirme ve üst üste koyma operasyonlarından sonra oluşturulur. Bir düzenli çözüm ağı oluşturucusu 3B kanat etrafında otomatik çözüm ağı oluşturabilmek için yeniden yapılandırılmıştır. Ardından, 3B HAD analizleri yine araştırma grubu tarafından geliştirilen bir HAD çözücüsü ile bu çözüm ağı üzerinde gerçekleştirilmiştir. Tasarım-çözüm döngüsü NASA Rotor-37 kompresör denek taşı sonuçları kullanılarak doğrulanmıştır. Geliştirilen yeni rotor kanatçıklarının Rotor-37 ile benzer basınç oranlarını sağladığı görülmüştür.
Anahtar Kelimeler: Orta-Çizgi Tasarımı, Parametrikleştirme, Radyal Eşitlik Teorisi, Çok Bloklu Yapısal Çözüm Ağı Üretimi, HAD, Eksenel Kompresör

INTRODUCTION

A gas turbine mainly consists of five components, which are the intake, compressor, combustion chamber, turbine, and the exhaust. The main function of the compressor in a gas turbine system is to increase the pressure of the working fluid before the combustion and the expansion processes. There are essentially three types of

compressors involving turbomachinery, which are axial, radial and mixed flow compressors. This study focuses on a design tool only for axial flow compressors. Axial flow compressors are generally employed in gas turbine engines since they can provide a higher pressure ratio and a larger flow rate for a given frontal area. They also demonstrate higher efficiency compared to other types of compressors.

Design of an axial flow compressor is an extremely critical stage in the development of gas turbine systems. The performance of an axial flow compressor has a direct effect on performances of both the combustion chamber and the turbine, since both are determined by the pressure ratio and mass flow rate supplied by the compressor. The flow through an axial compressor is 3D, transitional and turbulent. Moreover, separated flows and relatively thick boundary layer flows are observed at blade surfaces, hub and tip regions, as well as tip clearance flows, blade wakes and shock waves. A vast number of geometrical parameters are required to define the blade shape of an axial flow compressor. Some of them are blade camber, blade angles, blade row spacing, varying thickness distribution from the hub to the tip and from leading to trailing edge, stagger, skew, lean, twist, aspect ratio, hub/tip ratio, tip clearance and leading and trailing edge radii. Determination of all of these parameters makes the design of an axial flow compressor an extremely challenging task (Li, 2000).

An arbitrary blade design can be analyzed by solving flow equations around the compressor blades. To complete this task, Computational Fluid Dynamics (CFD) analysis of the flow around the blades of an axial flow compressor should be carried out by solving Navier-Stokes equations due to complexity of the flow. However, precise CFD analyses require large computer memory and CPU time. Therefore, these analyses are not suitable during the predesign stage of the axial flow compressor, a stage which requires many blade geometry candidates to be analyzed to achieve a blade design providing the desired compressor performance metrics. Therefore, 3D flow equations around the blade are simplified to 1D and 2D analyses by using numerous assumptions and empirical equations to rapidly eliminate

inadequate and inefficient designs. 1D analysis is the simplest one, is very fast and does not require large computer memory and CPU time. Therefore, the predesign of an axial flow compressor starts with 1D analysis, i.e. mean line design. Note that, 1D analysis contains too many assumptions and therefore, is not precise. Additionally, 1D analysis does not provide the blade geometry. Following 1D analysis, two different 2D analyses are performed in order to increase the fidelity and to obtain the main aspects of the blade geometry. 2D analyses are performed in two separate planes in the flow direction, which are called throughflow and blade-to-blade analyses.

Geometric parameters of blades are calculated with 2D analyses. Although throughflow and blade to blade analyses are more accurate, radial equilibrium theory is used to calculate these geometric parameters in this study. Then, blade geometry of the axial flow compressor are generated by utilizing these parameters. A 3D blade geometry is typically defined with Non-uniform rational basis spline (NURBS), B-spline or Bezier curves. These are parametric curves and require both a set of points and weight parameters associated to these points. Hence, the geometry of blades can be optimized easily by managing the parameters of these types of curves while satisfying the calculated geometric features of the blades. Finally, 3D Navier-Stokes analysis is performed after the generation of a high quality mesh around the designed blades. In this study, an aerodynamic design and analysis tool for axial flow compressors is developed. This tool consists of five parts, which are:

1. A mean-line design tool,
2. Geometry parametrization,
3. 3D blade geometry generation,
4. Block structured mesh generation around the blade,
5. An integrated 3D Reynolds Averaged Navier Stokes Solver (RANS)

The flow chart of the basic design cycle with the developed software is shown in Figure 1 (Xu, C. & Amano, R., 2008).
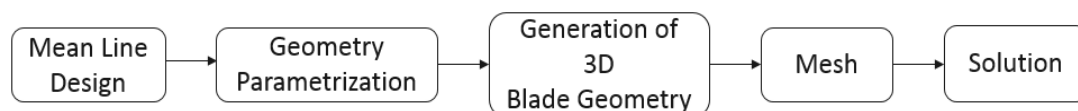
Figure 1. Compressor Design Flow Chart

The approach of the developed design analysis tool is different from available open-source axial compressor design tools, such as T-AXI (Turner et. al., 2007). Such tools limit the design and analysis process with 2D solvers. For example, T-AXI has an inline mesh generator and compressible flow solvers; all are implemented for 1D and 2D compressible and inviscid flows. The tool presented in this study allows a more

direct link to high accuracy 3D inviscid and viscous flow solvers, which permits an easy transition from the conceptual design to the final design of compressor stages. Also, our tool has the potential to be coupled with advanced shape optimization tools, due to its modular structure.

Developed design tool has the capability to design multistage axial compressor rotor-stator blades for a given pressure ratio. Transonic flow speeds are allowed. This study is limited to problems with relatively high pressure ratio per stage (around 2) and medium to large size axial compressors for thrust systems. For other applications of axial compressors, different correlations may be applied. CFD solutions are limited to single rotor stage calculations, since multistage calculations are not necessary at intended design phases.

Developed tool is validated using NASA Rotor-37 test case. Rotor 37 test case is a challenging test case constructed for validation of CFD solvers. Rotor 37 is an unusual 36-blade configuration, with rotational speed of 1800rad/s and pressure-ratio of 2.106. Experimental results are available for radial static and total pressure distributions as well as laser anemometry measurements within the rotor and the wake.

METHOD

Mean Line Design

Mean line analysis is a 1D analysis, which is based on common aerodynamic and thermodynamic principles. All the calculations are solved on mean line of the blade. Although many empirical equations are utilized in this analysis, its convergence is significantly rapid. Therefore, a lot of mean-line analyses can be performed in a short period of time to eliminate inadequate designs leading to low efficiency and/or are not suitable for the imposed design criteria. Hence, a new design study of a multi-stage axial flow compressor begins with a mean line design. This is the reason why the design toolkit developed in this study provides a mean-line analysis tool. Stage reactions are adjusted with flow angles at the exit of the stator, and pressure ratios are adjusted with stage load coefficients in the mean-line design part of the toolkit. A multistage axial flow compressor should be designed to comply with the performance requirements. The main performance metric used in this study is the pressure ratio. At the end of this analysis, flow and blade angles at mean-line of blades are calculated at the inlet and exit of the blade rows. In addition to that, blade spans are also calculated at these places.

Stage stacking method, which isolates each stage and analyze them consecutively, is utilized as the mean-line design algorithm. Firstly, calculations at the inlet are carried out using flow angle, mass flow rate, flow coefficient, hub to tip ratio and ambient conditions in a separate function. Then, calculated properties are utilized as the inlet conditions of the first rotor in the main stage loop. Next, flow properties between rotor and stator are calculated by assuming constant rothalpy between the inlet and exit of rotor. Flow properties at the exit of the stator are calculated by assuming constant total enthalpy between the inlet and exit of the stator. Then, these calculated flow properties at the exit of the stator are used at the inlet of the rotor of the following stage. These calculations are repeated until the last stage.

The flowchart of the mean-line design and analysis part is given in the Figure 2. Note that, Station 1 is located at the inlet of the rotor, Station 2 is located between the rotor and stator, and Station 3 is located at the exit of the stator. Up to this point, stage design is rather rudimentary where neither losses nor experimental correlations are applied. Calculation of incidence and deviation angles are based on empirical equations provided by NASA report NASA-SP36 (Johnson, I. A., & Bullock, R. D., 1965) (Aksel, 1985). Loss calculations are performed as suggested by Aungier (Aungier, 2003). Solidity of the blade rows are calculated through optimum solidity equation, which is suggested by Hearsey (Hearsey, 1986). Thermodynamic properties at each station are calculated by using empirical equations (McBridge, B.J., Gordon S. & Reno M.A., 1993).
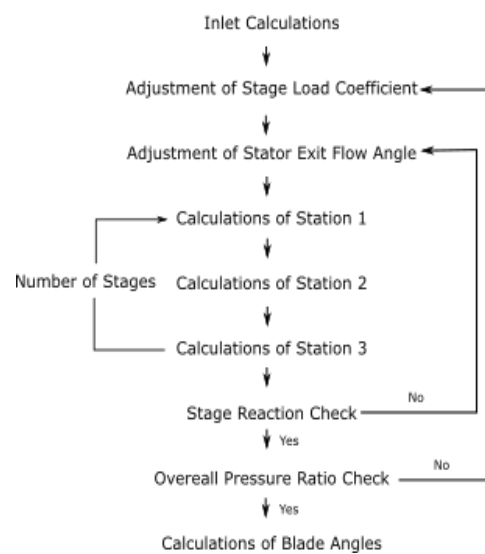
Figure 2. Mean Line Design Flow Chart

After completing the correction calculations described above, blade angles at the mean-line are calculated at the last step of the mean-line design. These angles should be calculated along the span of each blade to obtain the 3D blade geometry. Radial equilibrium theory, given by Equation 1, is used to obtain these flow angles at different radial positions of the blade span.

$$C_{t1} = aR^n - \frac{b}{R} \quad \text{(Rotor Inlet)}$$
$$C_{t2} = aR^n + \frac{b}{R} \quad \text{(Rotor Exit)} \tag{1}$$

where C_t represents whirl velocities along the blade span. a and b are constants.

$$a = u_m(1 - \Lambda_m)$$
$$b = \frac{C_{t2} - C_{t1}}{2}R$$

where Λ_m is the degree of reaction and n is defined as;

$$n = \begin{cases} -1 & \text{free vortex whirl distribution} \\ 0 & \text{exponential swirl distribution} \\ 1 & \text{constant reaction distribution} \end{cases}$$

181

and R is calculated as;

$$R = \frac{r}{r_m}$$

where r is the radial position on the blade and r_m is the mean radius of the blade (Mattingly, J. D., Heiser, W. H., & Daley, D. H., 1987) (Saravanamuttoo, H. I., Rogers, G. F., & Cohen, H., 2001).

Geometry Parametrization

At this point, flow angles and some geometric features of compressor blades are determined. It should be noted that the collected information about each blade is detailed, but not definitive. In other words, it is possible to construct multiple blade geometries with the collected information. Unsurprisingly, each blade construct will yield a different stage performance. The second objective is to derive a set of geometric parameters that will allow construction of blades and be easily adjusted when it is necessary.

Defining geometry using a minimal set of geometric and aerodynamic parameters is called parameterization. In this part of the developed tool, NURBS curves and its properties are used to define 2D blade cross-sections. Generated blades are always constructed by smooth blade surfaces. Also, the geometry can be quickly modified in the optimization tool by adjusting weights of control points of NURBS (Nemnem, 2014). A NURBS curve is calculated as;

$$C(t) = \frac{\sum_{i=0}^{n} N_{i,p}(t)\, w_i\, CP_i}{\sum_{j=0}^{n} N_{j,p}(t)\, w_j} \quad a \leq t \leq b \qquad (2)$$

where CP_i are control points, w_i are weights of corresponding control points and $N_{i,p}$ are the p-th degree B-spline basis function defined on the knot vector;

$$X = \left\{ \underbrace{a, \ldots, a}_{p+1}, u_{p+1}, \ldots, u_{m-p-1}, \underbrace{b, \ldots, b}_{p+1} \right\} \qquad (3)$$

where u_i's are called as knots and the knots can be considered as division points that subdivide the interval $[a,b]$ into knot spans. All basis functions are supposed to have their domain on $[a,b]$ and these basis functions, $N_{i,p}$, are calculated as;

$$N_{i,0}(t) = \begin{cases} 1 & if\ u_i \leq t \leq u_{i+1} \\ 0 & otherwise \end{cases}$$
$$N_{i,p}(t) = \frac{t - u_i}{u_{i+p} - u_i} N_{i,p-1}(t) + \frac{u_{i+p+1} - t}{u_{i+p+1} - u_{i+1}} N_{i+1,p-1}(t) \qquad (4)$$

Geometry parametrization part begins by approximating the hub and tip curves of the axial flow compressor with

cubic NURBS using the results of the mean-line design. Meridional curves are added between the hub and tip to obtain different cross-sections along the blade span. In addition to the hub and tip parametrization, camber line (Figure **3**), blade thickness distribution (Figure 4) and leading and trailing edge shape (Figure 5) are also parametrized by defining them with NURBS curves. 2D blade cross-sections through the blade span are generated with these parametrized curves. Then, all generated cross-sections are mapped onto corresponding meridional surface, generated by rotation of the meridional curve around the compressor rotation line. As a result, 3D blade cross sections are obtained and 3D blade geometry is generated by stacking up these 3D blade cross-sections (Koini G. N., Sarakinos S. S. & Nikolos I. K., 2009).
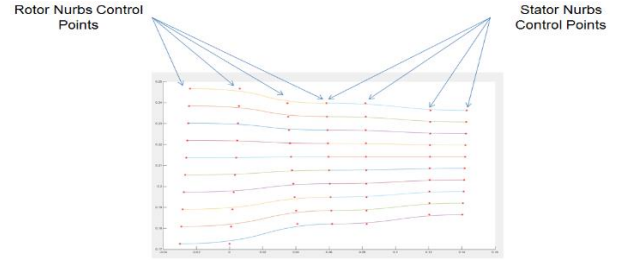
Figure 3. Parametrization of Meridional Curve
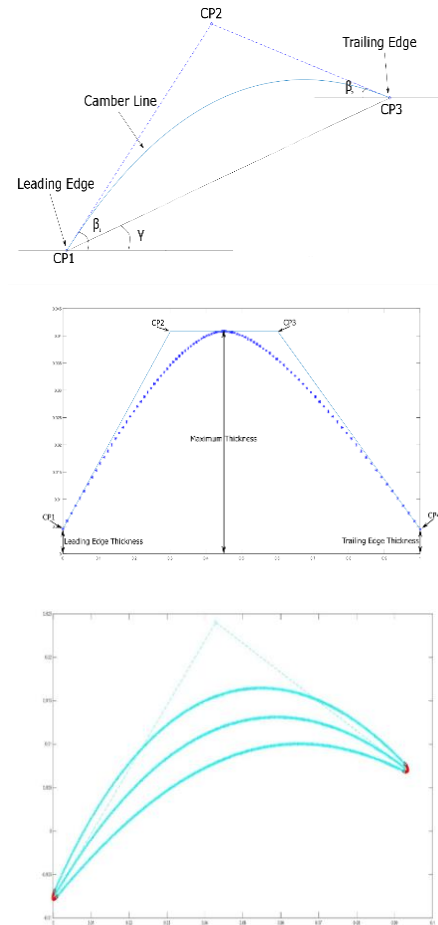
Figure 4. Parametrization of 2D Blade Cross Section
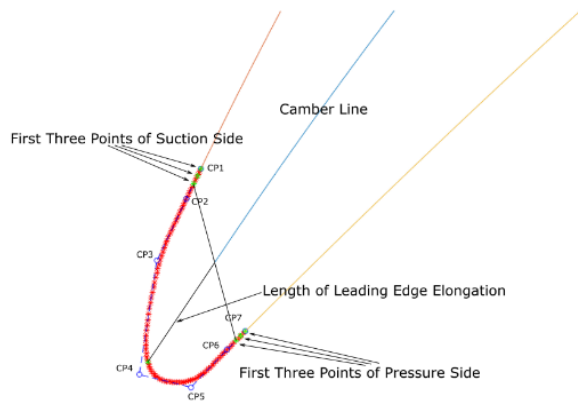
Figure 5. Leading Edge
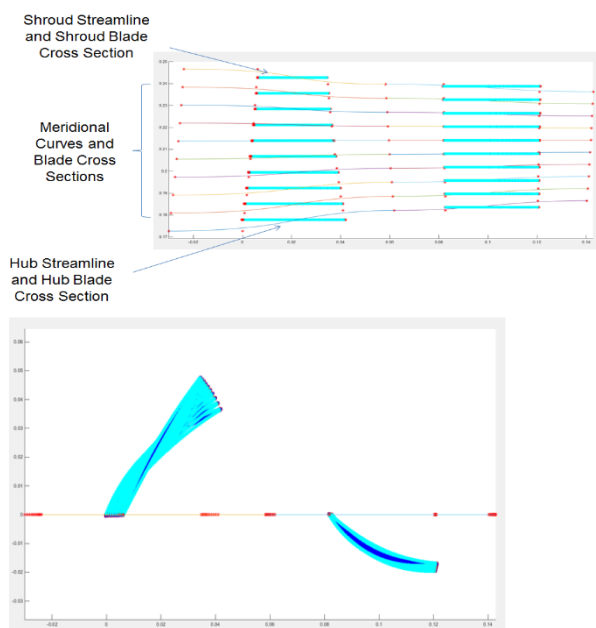
Figure 6. Meridional Curves and Corresponding Blade Cross Section

Figure 7. Mapping of 2D Blade Cross Section to Corresponding Meridional Curve and Result of Stacking Process

Automatic Multiblock Structured Mesh Generation

Multiblock structured mesh generation is the most suitable mesh generation technique for turbomachinery applications. A structured mesh that comply with the defined topology can be generated rapidly around the compressor blade. Moreover, reasonably satisfactory meshes can be obtained for different blade geometries easily and automatically. For this reason, a multiblock structured grid generation program is developed to generate mesh for the performance analysis of the 3D blade geometry. Two types of structured mesh generation methods, algebraic mesh generation and elliptic mesh generation, are included in the developed tool.

Algebraic mesh generation method is a mesh generation procedure based on transfinite interpolation. This method can be defined as the determination of grid point coordinates within the computational domain by interpolation from coordinates and derivatives of the specified points, located on the domain boundaries. This method is extensively used in CFD due to its ease of computation and capability of direct control over grid node locations. On the other hand, this method tends to preserve the features of boundaries. Hence, discontinuity in the slope of the boundary curves will generally propagate through the interior region. Therefore, generated grids are not always smooth. Projectors are used to determine the locations of internal grid points by interpolating specified boundary conditions in one dimension. These locations in two and three dimensions are found with the Boolean sum of projectors. All projector and Boolean sum operations are explained clearly by Farrashkhalvat and Miles (Farrashkhalvat, M., & Miles, J. P., 2003).

The second method, which is the elliptic mesh generation method, is based on the solution of quasi-linear partial differential equations given by Equation (5) in the computational domain using Dirichlet boundary conditions. In Equation (5), terms α_{ij} are scalar functions of $\vec{r}$ and P, Q and R are the control functions. This mesh generation method prevents the propagation of slope

183

discontinuity at the boundaries in the computational domain and generates a smooth mesh. Because of these advantages, firstly the computational mesh is generated with algebraic mesh generation method. Next, this mesh is used as a starting point in the elliptic mesh generation method to obtain a smooth mesh (Farrashkhalvat, M., & Miles, J. P., 2003) (Dener, 1992).

$$
\begin{aligned}
\alpha_{11}\vec{r}_{uu} + \alpha_{22}\vec{r}_{vv} &+ \alpha_{33}\vec{r}_{ww} \\
&+ 2(\alpha_{12}\vec{r}_{uv} \\
&+ \alpha_{13}\vec{r}_{uw} \\
&+ \alpha_{23}\vec{r}_{vw}) \\
&= -\alpha_{11}\vec{r}_u P \\
&- \alpha_{22}\vec{r}_v Q \\
&- \alpha_{33}\vec{r}_w R
\end{aligned} \tag{5}
$$
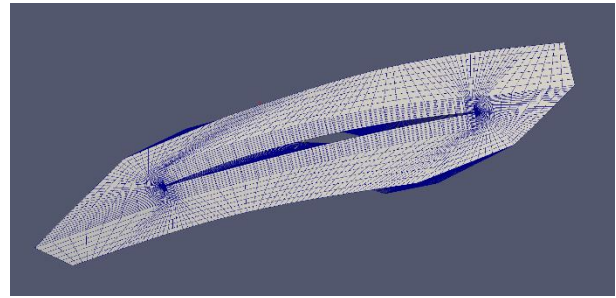
a) Algebraic mesh
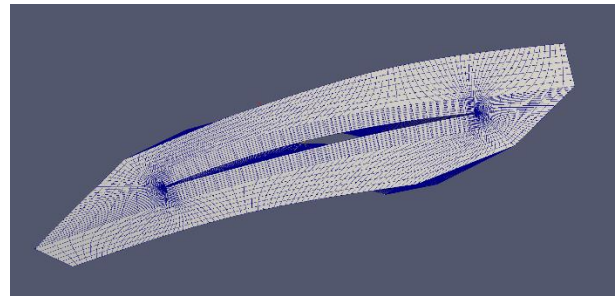
b) Elliptic mesh

Figure 8. Example of Algebraic Mesh and Elliptic Mesh
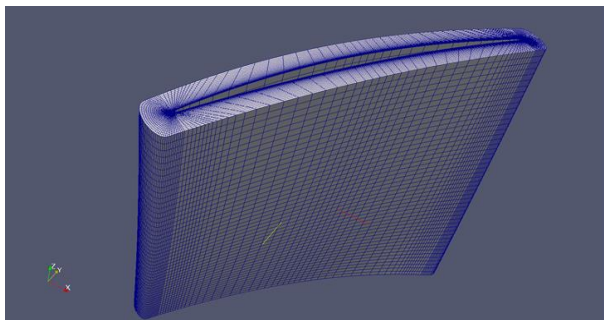
a)   Step 1
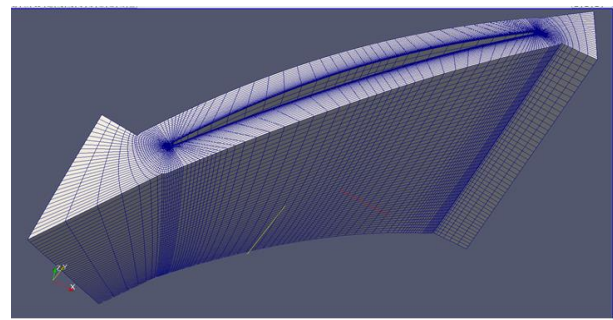
b)   Step 2
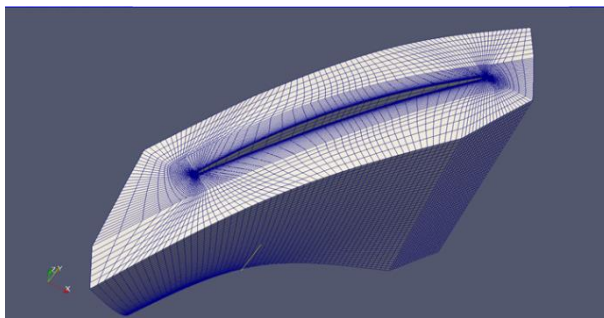
c)   Step 3
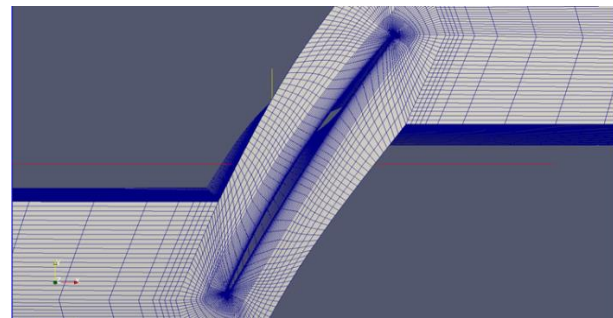
d)   Step 4

Figure 9. Automatic Mesh Generation

184
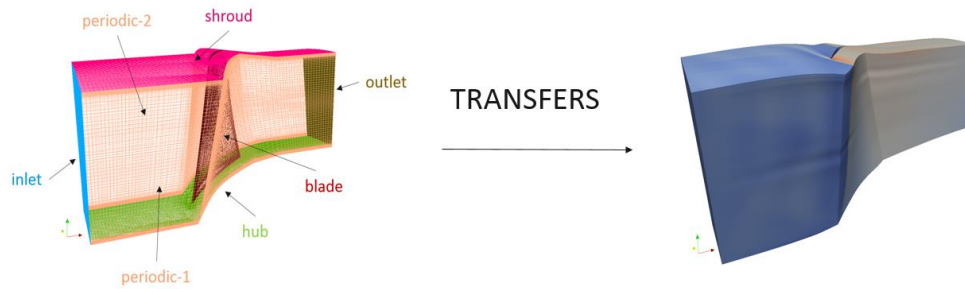
Figure 10. 3D CFD Analysis

The mesh is first generated by algebraic grid generation method and it is then smoothed by the elliptic grid generation method. In the mesh generation part, H-O-H mesh topology is used. First, a very high quality O-mesh is generated around the blade geometry to allow the calculations at the boundary layer region to be as accurate as possible. Then H mesh is created at the inlet, outlet, and both symmetry sides of the blade. The solution on this mesh is then performed by using an in-house developed solver with necessary boundary conditions at inlet, outlet, no-slip wall and symmetry surface. Inlet and outlet boundary conditions are taken from the design condition of the blade.

Solver

In-house CFD solver (TRANSFERS) is utilized to analyze the flow in multistage axial flow compressor blade passages. TRANSFERS is developed based on Loci framework. TRANSFERS uses finite volume procedure to discretize the flow equations and Spalart Allmaras, baseline (BSL), shear stress transport, hybrid RANS/LES (Large Eddy Simulation) turbulence models are implemented in the code.

RESULTS

Three test cases are performed for validation of the developed design and analysis tool.

Test case 1 aims the validation of both multiblock structured mesh generator and in-house CFD solver. For this purpose, the geometry of Rotor 37 is meshed and CFD simulations are performed. Then, CFD results and experimental results of Rotor 37 are compared.

Parametrization module of the design tool is validated by reconstructing Rotor 37 geometry in test case 2.

Test case 3 is constructed to validate the overall performance of the design and analysis tool. For this purpose, a new blade to comply with the design point of Rotor 37 is generated using the design tool and geometry of this blade is then constructed by using blade angles, chord lengths, blade thickness distributions as well as hub and shroud curves. CFD results of the new blade geometry are compared with the experimental results of Rotor 37. Therefore, the design part of the developed tool is validated with test case 3. In the second part of test case 3, a new compressor stage is designed to comply with the

design point of Stage 37. Subsequently, geometric properties and CFD results of new stage are compared with the geometric properties of Stage 37.

Verification of Mesher and Flow Solver

Rotor 37 test case is use d (Moore, R. D., & Reid, L., 1980) for the validation of structured mesh generator and in-house solver in test case 1. Mesh is generated for Rotor 37 blade automatically with the multiblock structured mesh generation code and this mesh is solved by using the in-house developed flow solver. BSL turbulence model (Menter, 1994) is utilized for the simulation of viscous flows. Solutions are compared with experimental results, and very good agreement is observed between CFD results and experimental results.
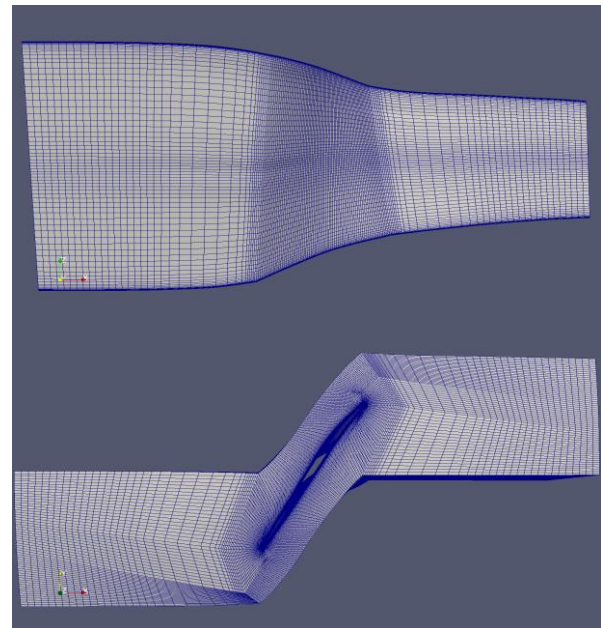
Figure 11. Rotor 37 Mesh: Symmetry surface view (top), shroud view (bottom)
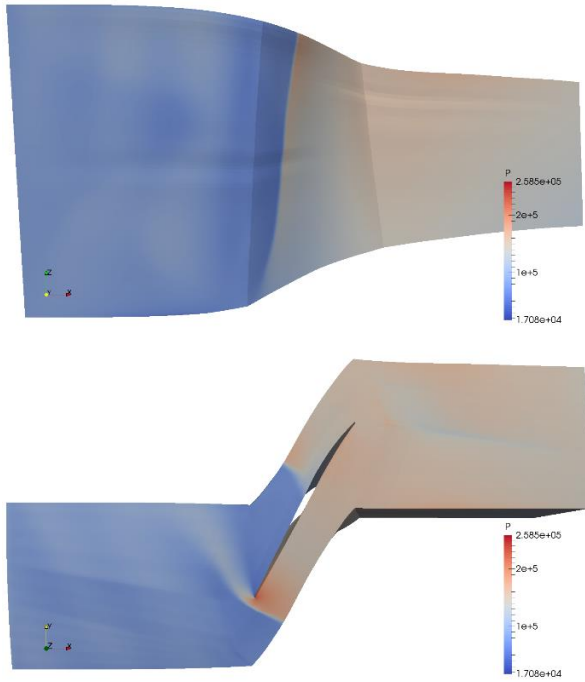
Figure 12. Rotor 37 Static Pressure Distribution on the flow channel boundaries of Rotor 37 geometry (Pout=131000Pa): Symmetry surface view (top), shroud view (bottom)
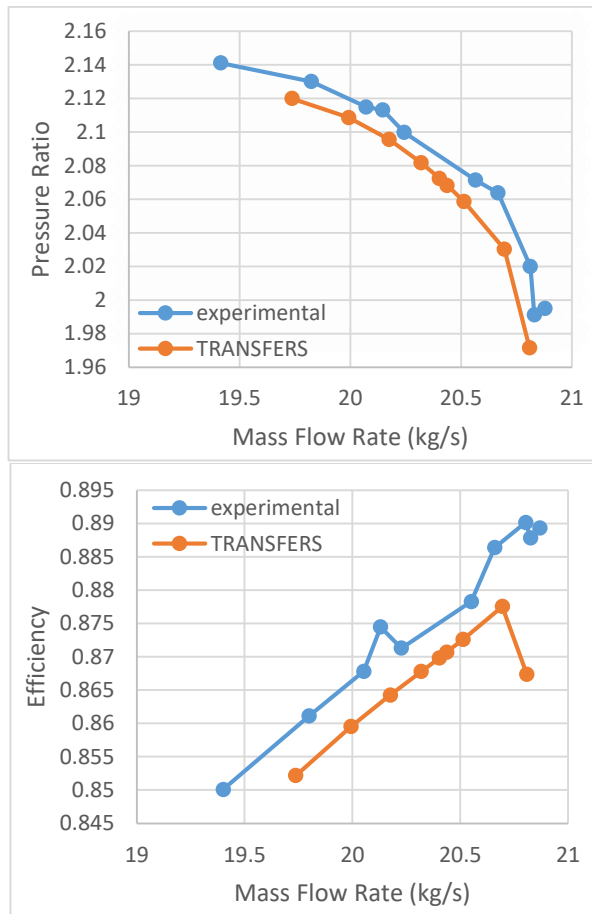
Figure 13. Comparison of CFD Solutions and Experiment Results for pressure ratio (top) and isentropic efficiency (bottom)
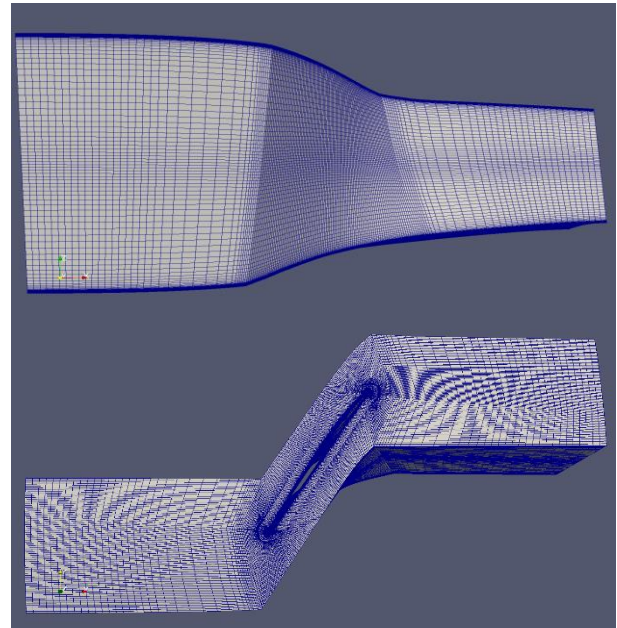
Figure 14. Parametrization Method Mesh: Symmetry surface view (top), shroud view (bottom)
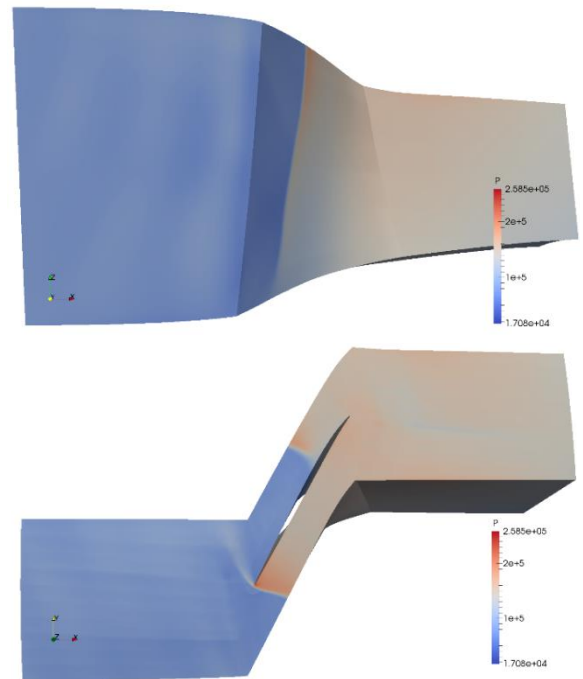
Figure 15. Pressure Distribution around the Parametrized Blade (Pout = 130000Pa): Symmetry surface view (top), shroud view (bottom)

Validation of Blade Parametrization

Parametrization method is also validated by using Rotor 37 in test case 2. Hub and shroud curves are taken from original Rotor 37 data. Also, blade cross sections are generated by using blade angles, chord lengths and blade thickness distributions of original Rotor 37 (Moore, R. D., & Reid, L., 1980). Unexpected results are obtained when the weight of mid control point of camber line NURBS is taken as 1.0. After then, this weight is increased to 1.5 and 2.0 successively. It is very difficult to observe the geometrical differences between original geometry and recreated geometry, as seen in Figure 11

and Figure 14. Also, simulation results are very similar, where the difference is observed at the center line of the blade cross sections. Remarkably similar results to the experimental results are obtained when this weight is taken as 2.0. All results are presented in Figure 16.
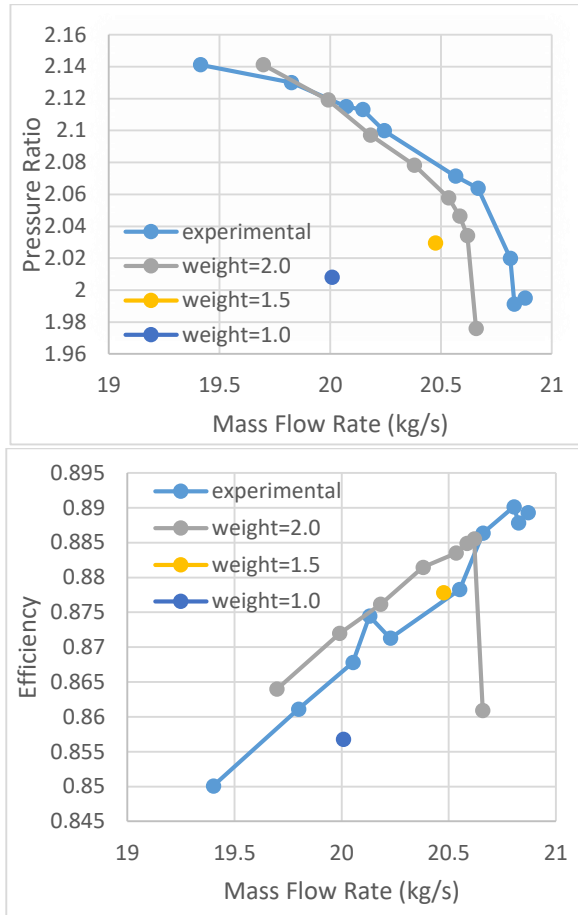
Figure 16. Comparison of Parametrized Blade CFD Solutions and Experimental Results for pressure ratio (top) and isentropic efficiency (bottom)

It should be noted that, this test case aims to clarify following questions:

    a) If the blade angles, chord lengths, thickness distribution and also hub and shroud curves can be calculated correctly

    b) If the 3D blade geometry can successfully be generated by the parametrization part of the tool

    c) If this geometry can easily be optimized by varying the weight of control points.

As seen above, parametrization tool coupled with the mesh generator and the solver can generate very similar blade with significantly different performances. Therefore, if an initial geometry is formed, many iterations of this basic geometry can be created to achieve a better performing compressor stage.

Validation of the Blade Design and Verification Cycle

In this part, a new axial compressor stage is designed to validate the blade-design part of the developed tool. Design parameters are chosen similar to Stage 37 in order to compare the new design geometry with the original Stage 37 geometry. This design is carried out by using free vortex whirl distribution. C series profile correlations (Aksel, 1985) are employed for the calculations of incidence and deviation angles. The design point of the new stage with the calculated number of blades at rotor and stator rows is given in Table 1.

Table 1. Design Point of the New Stage and Number of Blades

	New Design	Rotor 37
Pressure ratio of the rotor	2.11	2.106
Pressure ratio of the stage	2.08	2.05
Mass flow rate	20.188 kg/s	20.188 kg/s
Number of blades of the rotor	39	36
Number of blades of the stator	60	45

The calculated blade angles and other geometric parameters of the new designed rotor are given in Table 2 and Table 3, respectively with Rotor 37 data.

Table 2. Blade Angles

	New Design	Rotor 37
Shroud - Blade Inlet	63.73	62.53
Shroud - Blade Outlet	49.86	49.98
Shroud - Stagger	56.79	60.63
Mean - Blade Inlet	58.10	56.53
Mean - Blade Outlet	38.10	38.87
Mean - Stagger	48.10	53.39
Hub - Blade Inlet	51.44	52.04
Hub - Blade Outlet	17.74	16.75
Hub - Stagger	34.59	38.92

Table 3. Geometric Parameters

	New Design	Rotor 37
Shroud - Radius In	0.25	0.2523
Shroud - Radius Out	0.243	0.245
Shroud – Chord	0.0561	0.05592
Mean - Radius In	0.216	0.2176
Mean - Radius Out	0.216	0.2162
Mean – Chord	0.0561	0.05570
Hub - Radius In	0.175	0.1778
Hub - Radius Out	0.185	0.1873
Hub – Chord	0.0561	0.05627
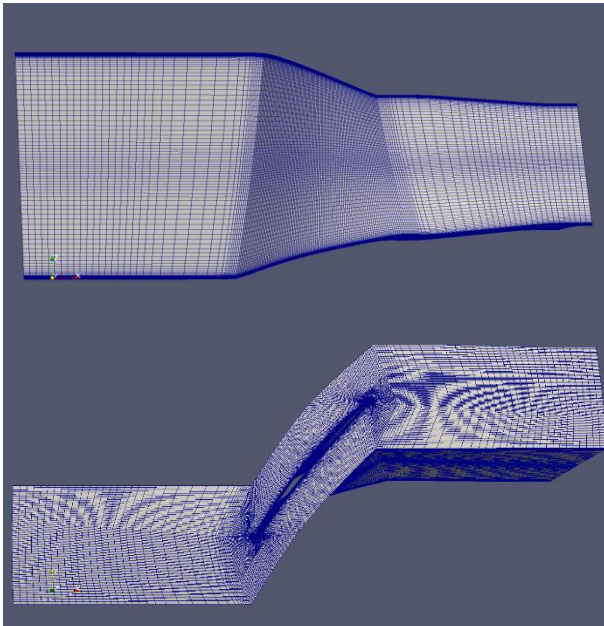
Figure 17. Mesh around the Designed Rotor: Symmetry surface view (top), shroud view (bottom)
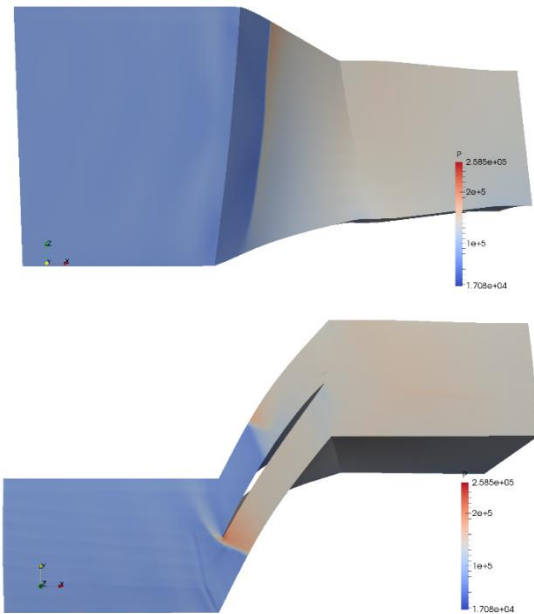
Figure 18. Pressure Distribution around Designed Rotor (Pout = 130000Pa), Symmetry surface view (top), shroud view (bottom)
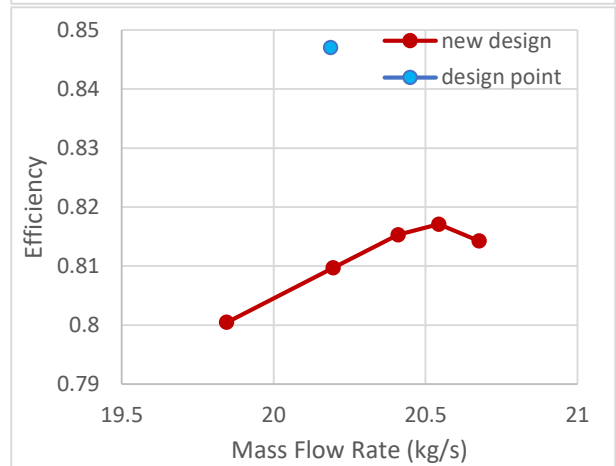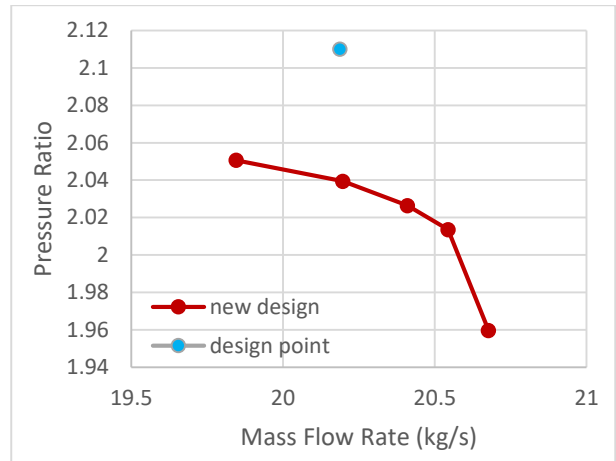
Figure 19. Performance Map of New Designed Rotor for pressure ratio (top) and isentropic efficiency (bottom)

The design of the new blade is very different than the Rotor 37, which is shown in Figures 11 and 14. The number of blades are 39 instead of 36, which results in narrower flow channel as seen in Figure 17. It should be noted that experimental rotor 37 has an unusual choice of number of blades, since the number of blades at each row is selected as odd numbers to reduce the risk of resonance. Our blade is designed with this rule in mind. Calculated blade angles are similar to the original blade angles of Rotor 37. However, the performance of the designed blade at the design point is less than expected, the value of which is calculated by the mean-line design module. This is justified by comparing total pressure distributions at the outlet boundary. Note that these distributions are calculated using the same boundary conditions.

Distribution of the total pressure on the hub side of the new design is similar to the pressure distribution of Rotor 37. However, total pressure distributions on the shroud side are different from each other. It is seen that the newly designed rotor results in less total pressure rise at the shroud side of the stage.

188

(a) Rotor 37

b) Parametrized Geometry

(c) Rotor of New Design
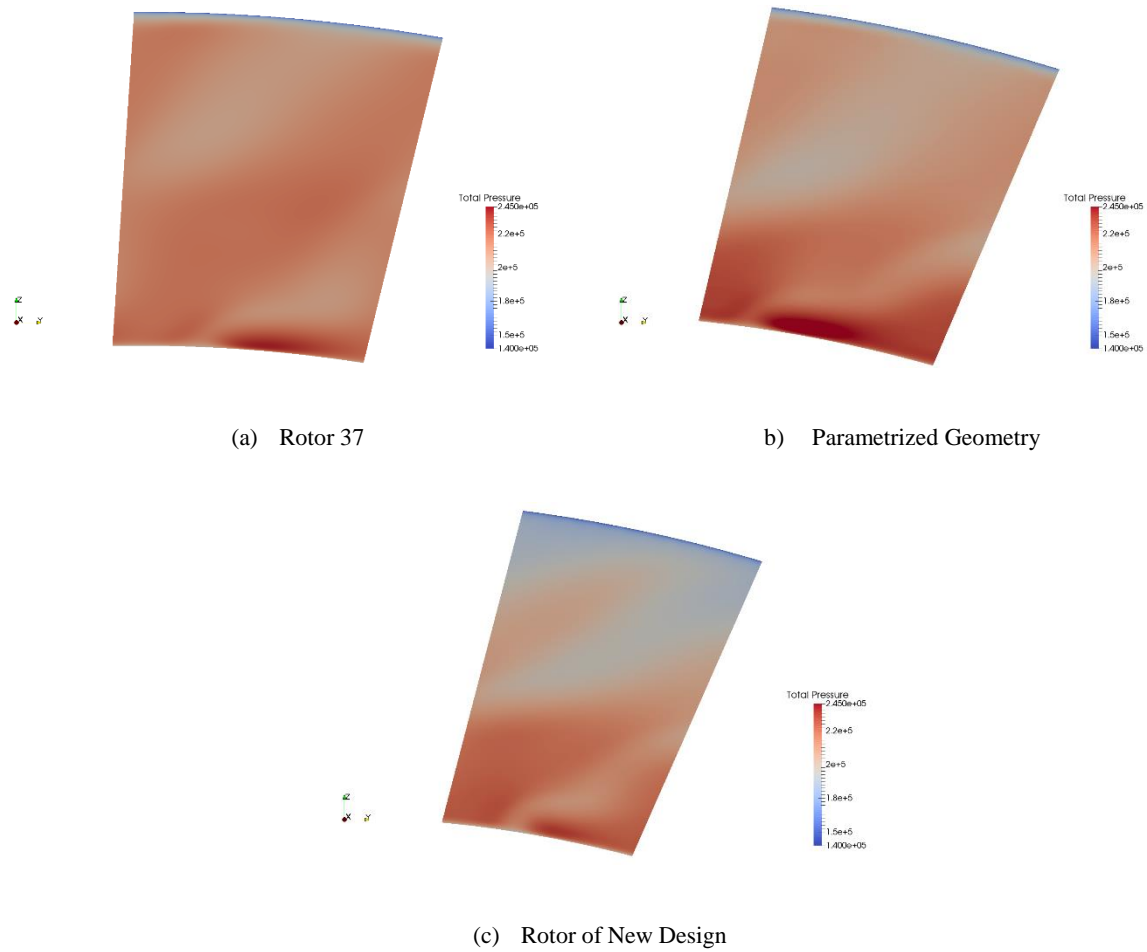
Figure 20. Total Pressure Distribution at Outlet Boundary

Finally, analysis of the new stage is carried out after the rotor analysis. In-house CFD solver does not contain mixing plane boundary condition for analyzing a stage with one blade passage. Hence analysis of this stage is performed by solving all blade passages, but through only on the mean line cross section by considering time and CPU cost. The calculated blade angles and other geometric parameters of this cross-section of this stage and Rotor 37 are given in Table 4.

Table 4. Blade Angles and Geometric Parameter of Mean Cross Section of Designed Stage and Rotor 37

	Blade Inlet Angle (°)	**Blade Outlet Angle (°)**	**Stagger Angle (°)**	**Chord (m)**
	Rotor			
New Design	58.11	38.03	48.10	0.0561
Stage 37	56.56	38.87	51.16	0.0557
	Stator			
New Design	46.60	6.81	26.7	0.0432
Stage 37	42.12	2.54	22.64	0.04049
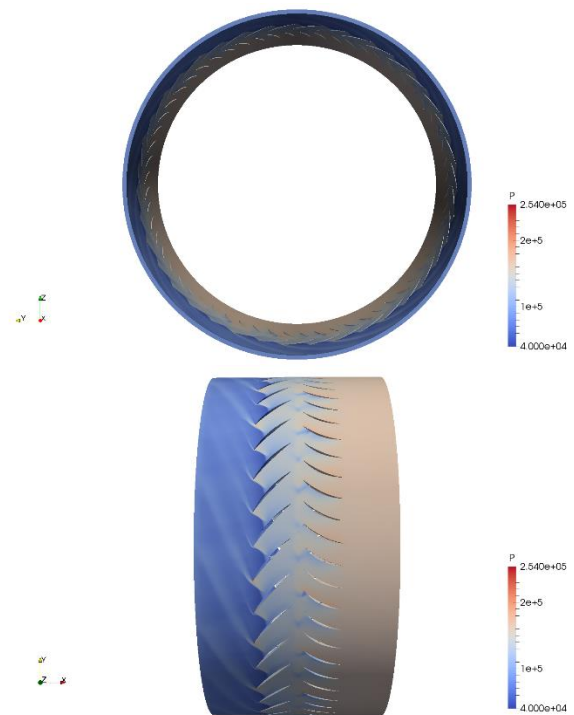
Figure 21. 3D View of Pressure Distribution of Designed Stage (Pout=160000 Pa) Side view (top) and axial view (bottom)
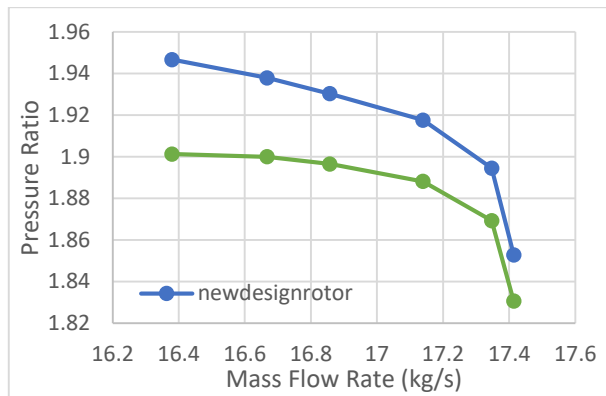
Figure 22. Performance of Designed Stage

CONCLUSION

In this study, an automatic design and analysis tool for axial flow compressors is developed. This tool consists of mean-line design, parametrization, 3D blade geometry generation, mesh generation, and flow solver modules. Validation of the mesh generator and in-house solver are carried out by using Rotor 37 geometry. Calculated CFD results are found to be similar to the experimental results of Rotor 37. Then Rotor 37 geometry is reconstructed with the parametrization module. For this purpose, blade cross sections are generated by parametrization part of the tool and the validation of this part is performed. Flow simulations around the parametrized blades show that, if the blade angles and chord lengths are calculated correctly, numerous cross sections can be generated successfully with this tool. In addition to that, these cross sections can be optimized by exploiting the properties of the NURBS curves. Design component of the tool is validated in test case 3 and a new stage is designed according to the design point of Rotor 37. The calculated geometric properties are remarkably close to original Rotor 37 geometry. However, CFD results of the new design do not conform to the design point. This is due to the fact that the required total pressure rise cannot be obtained on the downstream of the blade. Therefore, design component of the developed tool should be improved at blade sections close to the shroud to achieve better stage designs. It should be noted that, radial equilibrium theory is employed to calculate flow angles along the blade span in the developed tool. This elementary theory includes several assumptions. Better results can be achieved by using throughflow and blade-to-blade analyses to obtain these angles and blade thickness distributions. These tools are planned to be integrated to the main toolkit in the next versions of the developed software.

REFERENCES

Aksel, M. H. (1985). Eksenel Kompresörlerin Matematik Simülasyon Yolu ile Performanslarının Saptanması. Ankara: TÜBİTAK.

Aungier, R. H. (2003). Axial Flow Compressors: Strategy for Aerodynamic Design and Analysis. ASME Pres.

Dener, C. (1992). Development of an Interactive Grid Generation and Geometry Modeling System with Object Oriented Program. Doctoral Thesis.

Farrashkhalvat, M., & Miles, J. P. (2003). Basic structured grid generation with an introduction to unstructured grid generation. Oxford: Butterworth Heinemann.

Hearsey, R. M. (1986). Practical compressor aerodynamic design. In Advanced topics in turbomachinery design.

Johnson, I. A., & Bullock, R. D. (1965). Aerodynamic Design of Axial Flow Compressors, NASA SP-36. Washinghton D.C.: National Aeronautics and Space Administration.

Koini G. N., Sarakinos S. S. & Nikolos I. K. (2009). A Software Tool for Parametric Design of Turbomachinery Blades. Advances in Engineering Software, 41-51.

Li, Y. (2000). Three – dimensional flow and performance simulation of multistage axial flow compressors. Cranfield University.

Mattingly, J. D., Heiser, W. H., & Daley, D. H. (1987). Aircraft engine design. Washington, D.C.: American Institute of Aeronautics and Astronautics.

McBridge, B.J., Gordon S. & Reno M.A. (1993). Coefficients for calculating thermodynamics and transport properties of individual species. NASA.

Menter, F. R. (1994). Two equation eddy-viscosity turbulence models for engineering applications. AIAA Journal, 32(8) : 1598-1605.

Moore, R. D., & Reid, L. (1980). Performance of a single stage axial-flow transonic compressor with rotor and stator aspect ratios of 1.19 and 1.26, respectively, and with design pressure ratio of 2.05. Washington, DC: National Aeronautics and Space Administration.

Nemnem, F. (2014). A General Multidisciplinary Design Optimization System Applied to a Transonic Fan. University of Cincinnati.

Saravanamuttoo, H. I., Rogers, G. F., & Cohen, H. (2001). Gas turbine theory. Harlow. England: Prentice Hall.

Xu, C. & Amano, R. (2008). Design and optimization of Turbo compressors. Thermal Engineering in Power Systems WIT Transactions on State of the Art in Science and Engineering, 305-348.